10th International Conference on Fracture Mechanics of Concrete and Concrete Structures
FraMCoS-X
G. Pijaudier-Cabot, P. Grassl and C. La Borderie (Eds)
https://doi.org/10.21012/FC10.235504

TOWARD A FULLY COUPLED THM MESOSCOPIC MODELLING OF THE BEHAVIOUR OF CONCRETE AT HIGH TEMPERATURE

D. DAUTI[*], M. BRIFFAUT[*] AND S. DAL PONT[*]

[*]Univ. Grenoble Alpes, CNRS, Grenoble INP, 3SR,
F-38000 Grenoble, France
e-mail: matthieu.briffaut@3sr-grenoble.fr, stefano.dalpont@3sr-grenoble.fr

Key words: THM model, high temperature, concrete drying, mesoscopic, neutron tomography

Abstract: The exposure of concrete to fire, which often leads to spalling, is a phenomenon that is not yet fully understood. Given the complexity of the thermo-hydro-mechanical phenomena and their strong interaction, a combined numerical-experimental approach is indispensable for understanding the behaviour of concrete at high temperature with respect to spalling.
This study deals with the numerical modeling of moisture distribution in heated concrete, a parameter directly linked with spalling. The validation of these numerical models is usually based on experimental studies that monitor parameters such as gas pressure (P), temperature (T) and global mass loss (M). While such kind of experiments represent an important progress in better understanding the high temperature behaviour of concrete, some limitations appears due to the point-wise nature of temperature and gas pressure measurements. Firstly, the measurements might be influenced by the embedded sensors and secondly, the full-field information, which takes into account the role of concrete heterogeneity, is missing.

Recently, in-situ neutron tomography experiments for measuring the distribution of moisture content in 3D have been performed. Local information obtained in this experimental study provided valuable insight to benchmark the modelling.

In a first part of the paper, a homogenized continuum model has been employed for investigating various aspects, such as: speed of the drying front, moisture accumulation behind this front, experimental boundary effects etc. In a second part, a fully coupled 3D thermo-hydro-mechanical (THM) model is presented and used for simulating an experiment with a single aggregate for the purpose of investigating the influence of the aggregate on the drying front.

Numerical results clearly highlight the coupling between mechanical damage on the drying front progression and built the first step toward the simulation on the concrete behaviour at high temperature taking into account the heterogeneous nature of the concrete (mesoscopic simulations).

1 INTRODUCTION

The evolution of moisture content in heated concrete is an important parameter, which is believed to have a direct influence in fire spalling of concrete [1, 2]. The latter is a phenomenon which compromises the safety of concrete structures (e.g. tunnels, high-rise buildings etc.) as it exposes the reinforcement steel to high temperature and results in a reduced cross section of the concrete element. Despite the extensive research dedicated to spalling, this phenomenon is not yet fully understood due to the complex behaviour of concrete at high temperature which involves heat and mass transfer, known as thermo-hydric (TH) processes, as well as mechanical processes. State-of-the-art numerical models that take into account the coupled thermo-hydro-mechanical (THM) behaviour have been presented in literature [3, 4, 5, 6]. While the existing models are usually validated against standard measurements of temperature, gas pressure and global mass loss, neutron imaging proved to be an effective method for investigating the evolution of moisture content in real time in concrete while being heated [7, 8]. Indeed, local information obtained in such kind of experimental study provided valuable insight on several aspects, such as the influence of the aggregates size on the evolution of the moisture content and the moisture accumulation behind the drying front.

The objective of this work is the investigation of aggregates' influence on drying of concrete. For that purpose, a 3D mesoscale model that takes explicitly into account the concrete components (aggregates, cement matrix etc.), in other words the heterogeneity of concrete, is needed. In literature, Xotta et al. [9] have presented a THM model in the mesoscale. However, in that study the transport phenomena in concrete are described by a single fluid phase model. In the present study, a full multiphase THM coupled model will be used for performing mesoscopic analyses. In Section 2, the neutron tomography experimental data that have been used in this study for verification of the numerical model are summarized. In Section 3, the mathematical model used for the simulating the behavior of the concrete as a homogeneous (Section 3.1) but also as a heterogeneous material (Section 3.2) is presented. Then, in Section 4 the numerical analysis is presented. In Section 4.1, a 2D homogenized continuum model is used for simulating the temperature and moisture distribution measured experimentally and in section 4.2, 3D simulation using a mesoscopic modelling strategy with one aggregate for performing a simplified analysis of an aggregate influence on the drying front is presented.

2 EXPERIMENTAL RESULTS : NEUTRON TOMOGRAPHY

The experiments performed by Dauti et al. [10] consisted of heating tests performed inside a neutron beamline for the purpose of tracking the evolution of the moisture content while concrete was being exposed to high temperature (fig1).

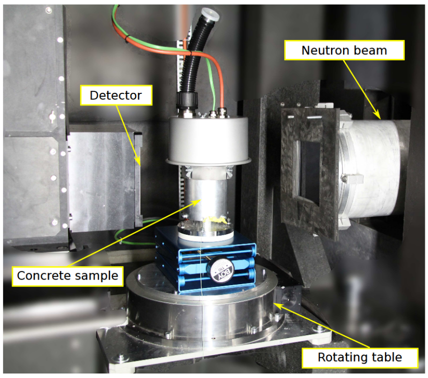

Figure 1: Setup (design during a collaboration between EMPA and 3SR lab) in the NeXT (D50) beamline at Institut Laue Langevin (ILL).

Cylindrical specimens with diameter 3 cm were tested with maximum aggregate size of 4 mm (HPC 4mm) and the other with 8 mm (HPC 8 mm). The overall volume of aggregates was the same for both mixes. In addition, a sample HPC 4mm with a single aggregate near the heated surface was cast for a more direct investigation of the influence of the aggregate on the moisture migration. In Figure 2, vertical slices from 3D scans at three different times containing the samples axis of rotation are shown for three tested samples: HPC 8mm (left), HPC 4mm (middle), HPC 4mm with a single big aggregate at the top (right). The evolution of the drying front is evident in the images. These results show qualitatively, how the drying front moves faster in the sample HPC 8mm compared to HPC 4 mm. They also show how a single aggregate severely affects the test, accelerating the drying process and modifying its shape. A possible explanation of the differences in the drying front is heat-induced cracking and its dependency on the aggregate size. The more pervasive fracture network induced around the bigger aggregates would accelerate the drying process.

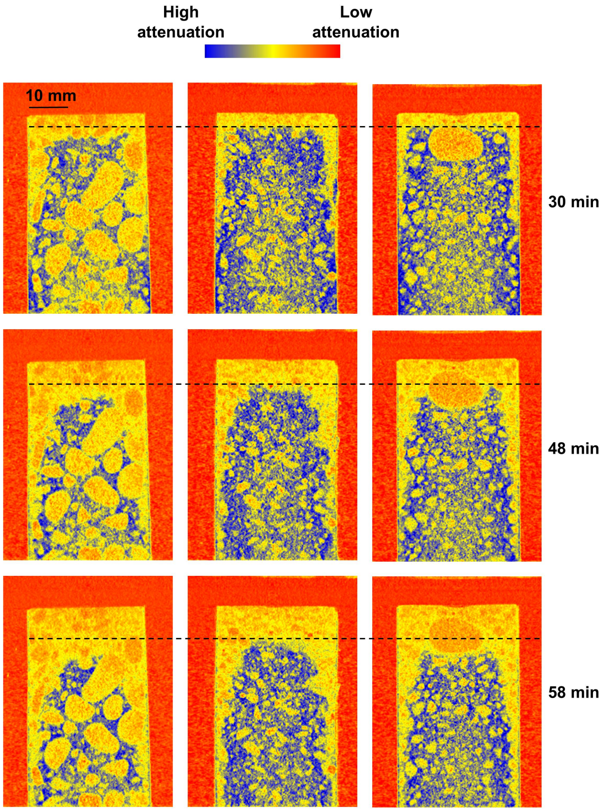

Figure 2: Vertical slices from reconstructed 3D volume showing the evolution of drying front

3 CONSTITUIVE TH MODELLING

The cementitious matrix is modeled as a porous multiphase material where the voids of the solid skeleton are filled with liquid and gas species. Perfect mixture theory between, dry air and water vapor is considered for the gas phase. Therefore, the hybrid mixture theory proposed by Lewis [11] is used. This one is based on the set of equation displayed in table 1 (indice a, l and v stands for air, liquid and vapor respectively) where ϕ is the porosity, S the saturation, ρ the density, t the time, T the temperature, K is the permeability, k_r is the relative permeability, p is the pressure, μ is the dynamic viscosity, M is the molar mass, D is the diffusion coefficient, C is the heat capacity, λ is the thermal conductivity, H is the enthalpy, m is the mass, g is the acceleration of gravity, t is the stress tensor.

Table 1: Set of equation of the Thermo-hydric modeling

The dry air balance equation

$$\phi(1-S_l)\left(\frac{\partial \rho_a}{\partial T}\frac{\partial T}{\partial t}+\frac{\partial \rho_a}{\partial p_c}\frac{\partial p_c}{\partial t}+\frac{\partial \rho_a}{\partial p_g}\frac{\partial p_g}{\partial t}\right)-\phi\rho_a\left(\frac{\partial S_l}{\partial T}\frac{\partial T}{\partial t}+\frac{\partial S_l}{\partial p_c}\frac{\partial p_c}{\partial t}\right)$$
$$+(1-S_l)\rho_a\frac{\partial \phi}{\partial T}\frac{\partial T}{\partial t}-\nabla\cdot\left(K\frac{\rho_a k_{rg}}{\mu_g}\nabla p_g\right)-\nabla\cdot\left(D\rho_g\frac{M_v M_a}{M_g^2}\nabla\left(\frac{p_a}{p_g}\right)\right)=0 \quad (1)$$

The water species (liquid-vapor) balance equation

$$(S_l\rho_l-(1-S_l)\rho_v)\frac{\partial \phi}{\partial T}\frac{\partial T}{\partial t}+S_l\phi\frac{\partial \rho_l}{\partial T}\frac{\partial T}{\partial t}+\phi(\rho_l-\rho_v)\left(\frac{\partial S_l}{\partial T}\frac{\partial T}{\partial t}+\frac{\partial S_l}{\partial p_c}\frac{\partial p_c}{\partial t}\right)$$
$$+(1-S_l)\phi\left(\frac{\partial \rho_v}{\partial T}\frac{\partial T}{\partial t}+\frac{\partial \rho_v}{\partial p_c}\frac{\partial p_c}{\partial t}+\frac{\partial \rho_v}{\partial p_g}\frac{\partial p_g}{\partial t}\right)-\nabla\cdot\left(K\frac{\rho_l k_{rl}}{\mu_l}(\nabla p_g-\nabla p_c)\right)$$
$$-\nabla\cdot\left(K\frac{\rho_v k_{rg}}{\mu_g}\nabla p_g\right)-\nabla\cdot\left(D\rho_g\frac{M_v M_a}{M_g^2}\nabla\left(\frac{p_v}{p_g}\right)\right)=-\dot{m}_{dehyd} \quad (2)$$

The energy balance equation

$$\rho C_p\frac{\partial T}{\partial t}-K\left(C_l\frac{\rho_l k_{rl}}{\mu_l}(\nabla p_g-\nabla p_c)+C_g\frac{\rho_v k_{rg}}{\mu_g}\nabla p_g\right)\cdot\nabla T-\nabla\cdot(\lambda\cdot\nabla T)=$$
$$-H_{vap}\dot{m}_{vap}+H_{dehyd}\dot{m}_{dehyd} \quad (3)$$

The linear momentum conservation equation

$$\nabla\cdot\left(\mathbf{t}^{Total}\right)+\rho\mathbf{g}=0 \qquad \text{where} \qquad \rho=(1-\phi)\rho_s+\phi S\rho_l+\phi(1-S)\rho_l \quad (4)$$

State variables are determined in the number of 3: gas pressure p_g, capillary pressure p_c, temperature T. The model takes into account all the main phenomena occurring in concrete at high temperatures such as phase changes, moisture transport (Fick and Darcy), etc Details about thermo-hydric modeling and constitutive equations used can be found in [12] The model has been implemented in the FE code Castem [13] and validated against available experimental tests measuring temperature, gas pressure and mass loss [14].

4 THM SIMULATIONS RESULTS

4.1 TH Homogeneous simulations (2D)

In experiments, the thermal boundaries conditions are not perfectly mastered. Indeed, only the temperature of the radiant heater is imposed but this one is not in contact with the specimen. Nevertheless thanks to samples with thermocouple, the boundaries conditions taken into account convection and radiation for the top part and convection for the lateral part have been calibrated (thermal and hydric insulation on the lateral surface is not perfect). Figure 3 display the evolution of the temperature measured by the thermocouples and the numerical results.

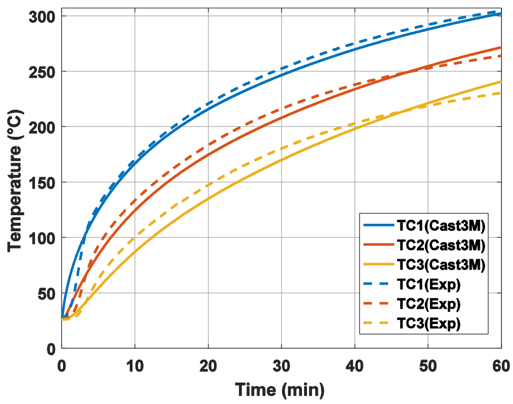

Figure 3: Results of thermal field calibration for three locations (3, 10, 20mm from the heated surface)

The pressure fields at different times are shown in Figure 4. The applied boundary condition results in a release of pressure at the lateral sides.

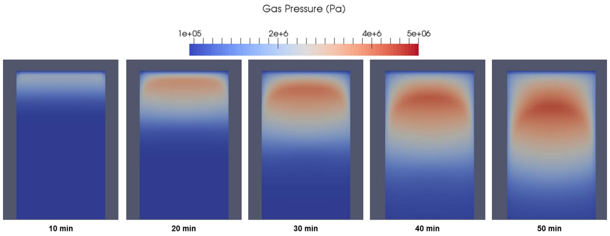

Figure 4: Non uniforme pressures field during experiment time

Temperature increase leads to an evolution of the moisture content in the cement paste due to physical processes such as dehydration, evaporation and condensation. In neutron tomography experiments, the attenuation coefficient (images grey value) is directly linked to the water content. Therefore, moisture profile can be evaluated though the change in grey value with respect to the initial stage. In numerical modelling, the variation in water content could be calculated from the evolution of the saturation of pores network and from dehydration of the cement paste. In order to compare the profile evolution, the numerical water content is normalized to the initial water content (figure 5). As in the experiments, one can observe a faster drying at the boundaries due to a possible lateral moisture escape. A moisture accumulation (black area in the picture) is predicted behind the front. In order to avoid the effect of imperfect boundary conditions, in both analyse, only the core of the specimen is considered. The comparison between experimental curves and numerical results is plotted in figure 6.

One can remark that the numerical model is able to predict the speed of the drying front (the plateau is well predicted) and that in both evolutions a moisture accumulation is observable (normalized water content superior to 1). This moisture accumulation seems to be more pronounced in the experiments. Nevertheless, as pointed out in [12], imaging artefacts due to beam hardening (evolving during time due to imperfect lateral moisture boundaries conditions) might affect the quantity of moisture accumulation obtained from image analysis.

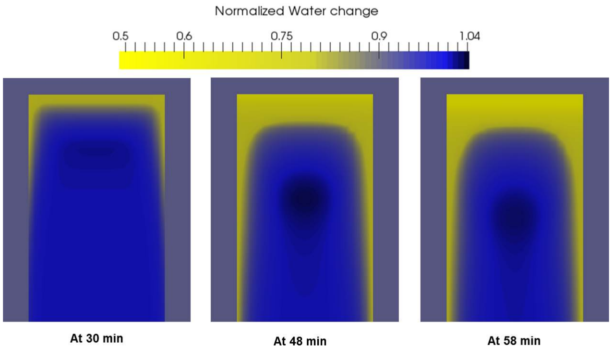

Figure 5: Results of the numerical simulations expressed in normalized water change

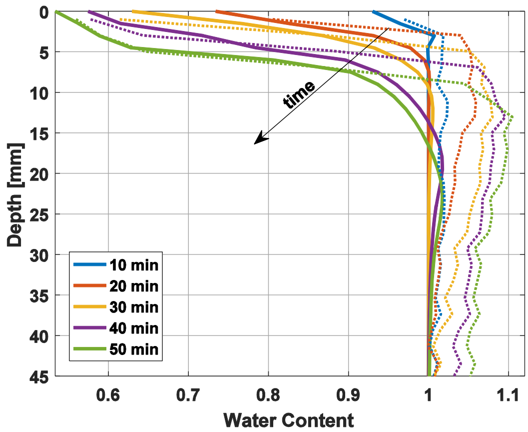

Figure 6: Moisture profil evolution: experiments in dotted lines and numerical simulation in solid lines

4.2 THM simulation Influence of the presence of aggregates: simplified mesoscopic approach

If the faster evolution of the drying from is obvious in the figure 2 due to the presence of a big aggregate, the higher thermal conductivity of the aggregate cannot explain the higher drying speed. Indeed a mesoscopic calculation based on a thermo-hydric-elastic calculation lead to only small difference in the temperature field (less to 5°C) and negligible difference in the pressure field (less to 0.2 MPa with respect to the maximal gas pressure obtained for the homogeneous calculation which was 3.2 MPa). The mesoscopic approach adopted for the case of HPC 4mm sample with a single aggregate at the top is illustrated on figure 7). Concrete is a bi-component material composed by large aggregates and the cementitious matrix with a perfect bond and without interfacial transition zone. Aggregates are modeled as an impermeable solid inclusion from a hydric point of view. They will therefore transfer heat but not mass. Thermo-mechanical behavior of each constituent has been explicitly considered with different coefficient of thermal dilation.

The results of the thermo-hydric-elastic calculation in term of normalized water content are displayed in figure 8.

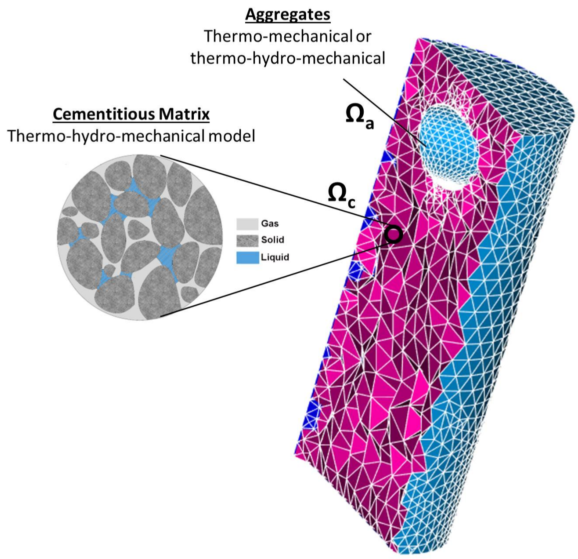

Figure 7: Vertical slices from reconstructed 3D volume showing the evolution of drying front

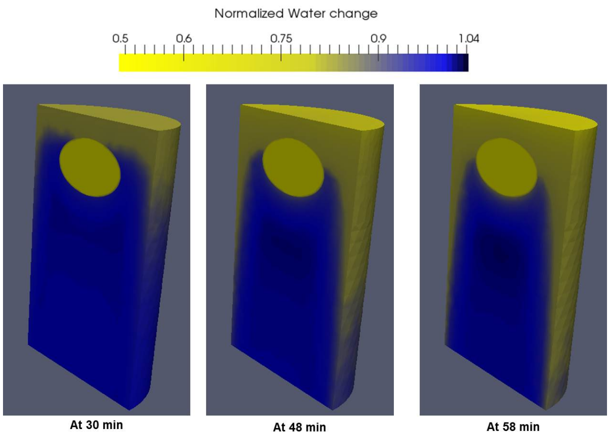

Figure 8: Vertical slices from reconstructed 3D volume showing the evolution of drying front

Consequently, thermo-hygro-mechanical simulations have been developed with a coupling between damage and permeability to capture the faster drying around the aggregate, which is likely to be caused by a more pervasive fracture network around the aggregate. Mechanical damage effects are taken into account by using the Mazars' scalar isotropic model in his non-local form [15].

The damage parameter is coupled with the permeability thanks to the relation proposed by Gawin [16].

$$k = k_0 \cdot 10^{A_T(T-T_0)} \cdot \left(\frac{p_g}{p_{atm}}\right)^{A_p} \cdot 10^{A_d d} \tag{7}$$

Where $k_0 = 10^{-20}\text{m}^2$, $AT = 0.005$, $A_p = 0.368$ and $A_d = 1$.

The obtained damage field due to the different thermal behavior of concrete component at high temperature (cementitious matrix tends to shrink due to dehydration whereas aggregate expand) is presented in figure 9 with the evolution of the normalized water evolution.

The evolution of the drying front seems is clearly impacted by the higher permeability closed to the big aggregate.

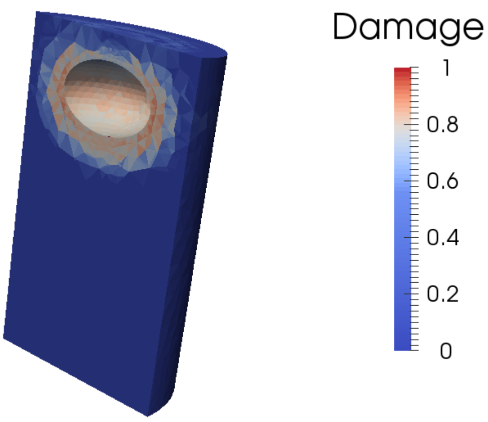

(a)

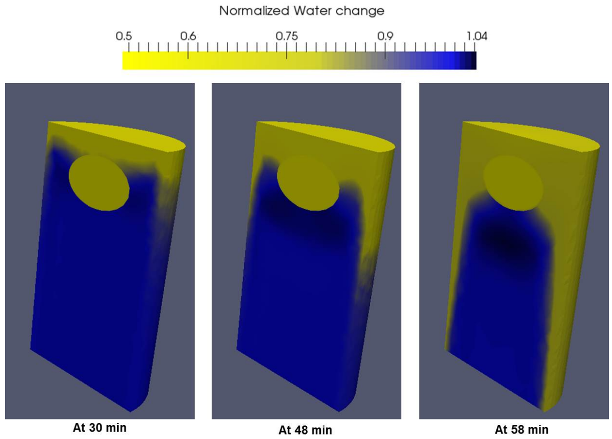

(b)

Figure 9: Damage field (a) and evolution of normalized water content for coupled THM model (b)

5 CONCLUSIONS

This contribution have present a numerical model implemented in Cast3M used for simulating neutron tomographies experiments on heated concrete.

After some calibrations due to the imperfect thermal and hydric boundaries conditions during the experiments, the model gives a good prediction of the drying speed of HPC composed with 8mm and 4mm aggregates. It also predicts a moisture accumulation, which is less compared to the experimental one. The model is also able to capture the lateral drying observed in the experiments when non-perfect boundaries conditions are used.

3D simplified mesoscopic simulation of an experiment with big a aggregate at the top have also been presented for the purpose of investigating the influence of the aggregate size on drying front. Thermo-hydro-mechanical simulations showed that the damage of the cementitous materials around the aggregated modify the shape of the drying front and the speed of its evolution. Such results is an important step toward a more complete mesoscopic analysis and gives some preliminary results for the physical interpretation of the faster drying in sample with bigger aggregate size.

ACKNOWLEDGEMENTS

This study was partially financed by LabEx TEC21.

REFERENCES

[1] D. Gawin, C. Majorana, B. Schrefler, Numerical analysis of hygro-thermal behaviour and damage of concrete at high temperature, Mechanics of Cohesive-frictional Materials 4 (1) (1999) 37–74.
[2] S. Dal Pont, H. Colina, A. Dupas, A. Ehrlacher, An experimental relationship between complete liquid saturation and violent damage in concrete submitted to high temperature, Magazine of Concrete Research 57 (8) (2005) 455–4
[3] R. Tenchev, L. Ly, J. Purkiss, Finite element analysis of coupled heat and moisture transfer in concrete subjected to fire, Numerical Heat Transfer Part A-applications 39 (2001) 685–710.
[4] C. T. Davie, C. J. Pearce, N. Biani, Coupled heat and moisture transport in concrete at elevated temperatures - effects of capillary pressure and adsorbed water, Numerical Heat Transfer, Part A: Applications 49 (8) (2006) 733–763.
[5] P. Kalifa, F.-D. Menneteau, D. Quenard, Spalling and pore pressure in HPC at high temperatures,Cement and Concrete Research 30 (12) (2000) 1915 – 1927.
[6]J.-C. Mindeguia, Experimental contribution to the understanding of the thermal instability risk of concrete, Theses, Université de Pau et des Pays de l'Adour (Jul. 2009).
[7] B. Weber, M. Wyrzykowski, M. Griffa, S. Carl, E. Lehmann, P. Lura, Neutron radiography of heated high-performance mortar, MATEC Web of Conferences 6 (2013) 03004.
[8] N. Toropovs, F. Lo Monte, M. Wyrzykowski, B. Weber, G. Sahmenko, P. Vontobel, R. Felicetti, P. Lura, Real-time measurements of temperature, pressure and moisture profiles in high-performance concrete exposed to high temperatures during neutron radiography imaging, Cement and Concrete Research 68 (2015) 166 – 1
[9] G. Xotta, G. Mazzucco, V. Salomoni, C. Majorana, K. Willam, Composite behavior of concrete materials under high temperatures, International Journal of Solids and Structures 64-65 (2015) 86– 99
[10] D. Dauti, A. Tengattini, S. Dal Pont, N. Toropovs, M. Briffaut, B. Weber, Analysis of moisture migration in concrete at high temperature through in-situ neutron tomography, Cement and Concrete Research 111 (2018) 41 –
[11] R. W. Lewis, B. A. Schrefler, The Finite Element Method in the Static and Dynamic Deformation and Consolidation of Porous Media, John Wiley,
[12] D. Dauti, S. Dal Pont, B. Weber, M. Briffaut, N. Toropovs, M. Wyrzykowski, G. Sciumè, Modeling concrete exposed to high temperature: Impact of dehydration and retention curves on moisture migration, International Journal for Numerical and Analytical Methods in Geomechanics 42 (13) (2018) 1516–1530
[13]CEA, Cast3M 15.0, Finite Element Software, http://www.cast3m.cea.fr
[14] S. Dal Pont, S. Durand, B. Schrefler, A multiphase thermo-hydro-mechanical model for concrete at high temperatures—Finite element implementation and validation under LOCA load, Nuclear Engineering and Design, vol. 237, 22, 2007, 2137-2150.
[15] G. Pijaudier-Cabot, Z. Baˇzant, Nonlocal damage theory, Journal of Engineering Mechanics – ASCE, 113 (10) (1987) 1512–153
[16] D. Gawin, F. Pesavento, B. Schrefler, Modelling of hygro-thermal behaviour of concrete at high temperature with thermo-chemical and mechanical material degradation, Computer Methods in Applied Mechanics and Engineering 192 (1314) (2003) 1731